Fracture behavior of welded steel bridge components

Khaled M. Mahmoud[1]

ABSTRACT | This paper presents the investigation of fracture behavior of welded steel bridge components. The interaction between a macroscopic crack and continuously distributed microscopic damage in a power-law hardening material is studied by accounting for void accumulation in the vicinity of the crack-tip. The damage is assumed to be concentrated to a small circular zone centered at the crack-tip, where growth and coalescence of microvoids are invoked. A component, loaded in Mode-I under plane strain condition, is considered. The deformation theory of plasticity is employed to obtain the stress, strain and displacement fields ahead of the tip of the crack, where a damage variable, D, is introduced to describe the mechanical effect of distributed microscopic damage. Only isotropic damage is considered in this paper. For monotonic loading, the external applied stress for small-scale and large-scale yielding solutions is found to be proportional to $a_0^{-1/(n+1)}$, where a_0 is half the initial crack length and n is the strain-hardening exponent of the material. This reduces to Griffith's classical result for elastic material. For fatigue crack propagation under small-scale yielding, the effects of initial crack size, final crack size and the cyclic stress level on the service life of welded steel bridge components are assessed and found to be in good agreement with Paris power-law for fatigue crack growth.

KEYWORDS | fracture behavior, bridge components, damage mechanics, microvoids, Mode-I, HRR singularity.

1 Introduction

Among the major concerns of bridge engineers is the fracture behavior of steel bridge components. Linear elastic fracture mechanics is a well-established tool in describing the fracture behavior of bridge structures, [1]. Conventional fracture approach deals only with the effect of a macroscopic crack in a defect free continuum. However, in reality, both a macroscopic crack and microscopic damage may exist simultaneously in a bridge component. Thus, the resulting load carrying capacity will be lower than in the case with only a macroscopic crack or with microscopic damage. Continuum damage mechanics describes the effect of continuously distributed microscopic damage. The continuum damage theory was first conceived for creep rupture studies, [2]. To investigate the interaction between a macroscopic crack and microscopic damage of a material with a nonlinear hardening stress-strain relationship, a combination of the two approaches has been considered in [3] and [4]. In the present paper, this interaction is applied to describe the fracture behavior of bridge steel. A stationary crack subjected to tensile loading (mode-I) under plane strain conditions is considered. Accurate determination of the stress, strain and displacement fields near the crack-tip is of a paramount importance in the development of sound fracture criteria. For a power-

1. Associate and Director of Long Span Bridges, Hardesty & Hanover, 1501 Broadway, Suite 310, New York, N.Y. 10036, U.S.A. Tel. (212) 944-1150, Fax (212) 391-0297. E-mail: kmahmoud@hardesty-hanover.com

law hardening plastic material, the crack-tip possesses the Hutchinson-Rice-Rosengren (HRR) singularity, [5] and [6].

A damage variable, D, which represents the remaining load bearing area of the cross-section, is introduced to describe the mechanical effect of distributed microscopic damage. Damage is usually an anisotropic phenomenon, however, only isotropic damage is considered in this paper. The assumption is quite reasonable due to the isotropy of steel. The one-dimensional representation of damage, considered here, is valid even with the "local approach to fracture." It should be noted, however, that the onset of localized deformation is not included in this paper. The damage, which is assumed proportional to the crack opening displacement, is confined to a small zone centered at the crack-tip. In this zone, the HRR asymptotic solution is modified to include the effect of damage. The conditions that characterize crack growth under monotonic and cyclic loadings are studied.

A brief summary of the basic mathematical equations of the HRR field, modified to include the effect of damage, is introduced. The shape effect in the process zone is thought to be of secondary order. However, guided by the results obtained by Mahmoud and Kassir, [4], a circular damage-zone, centered at the crack-tip is postulated. The criterion for initiation of crack instability for the small-scale yielding and large-scale yielding solutions is developed. The remotely applied stress, σ_∞, is found to be proportional to $a_0^{-1/(n+1)}$, where a_0 is half the initial crack length and n is the strain-hardening exponent of the material. This reduces to Griffith's classical result for elastic material (n=1). The application of the small-scale yielding solution to assess fatigue crack propagation due to tensile cyclic loading is also examined. The variations of the normalized crack length with the number of cycles required for failure are graphically exhibited, for given material parameters. The effect of initial and final crack size as well as the effect of cyclic stress level are investigated and found to be in very good agreement with Paris power-law for fatigue crack growth.

2 Basic equations

With the assumed isotropic damage, the variable, D, which describes the mechanical effect of damage is a scalar defined in [2] as:

$$D = A_{void} / A = 1 - (A_{net} / A) \quad \text{.....(1)}$$

where A and A_{net} are the macroscopically observable original and net cross-sectional areas respectively, while A_{void} is the cross-sectional area occupied by voids, $0 \le D \le 1$. It follows that the nominal stress, σ, and the actual stress, s, are related as:

$$\sigma = s(1 - D) = \Omega\, s \quad \text{.....(2)}$$

where Ω is the continuity function. It is assumed that the damage accumulation is concentrated in a small zone centered at the crack-tip, and referred to as the damage-zone. For a strain-hardening material, obeying a linear relation to the yield point (σ_0, ε_0) and a power-hardening law thereafter. Thus, the strain is related to the nominal stress, σ, according to:

$$\varepsilon = (\varepsilon_0 / \sigma_0)\,\sigma \quad , \quad \sigma < \sigma_0 \quad \text{.....(3a)}$$

$$\varepsilon = \varepsilon_0\,(\sigma / \sigma_0)^n \quad , \quad \sigma > \sigma_0 \quad \text{.....(3b)}$$

where σ_0 and ε_0 are reference stress and strain, respectively, and n is the power hardening exponent. The reference stress is a material parameter and may be considered as the yield stress.

Inside the damage-zone, the measure of damage is assumed to vary linearly with the crack opening displacement, i.e. $D = \lambda u_y$, where λ is a material damage parameter and u_y is the displacement normal to the crack plane. u_y shouldn't be confused with δ_t, the crack-tip opening displacement (CTOD). Within the zone, the net stresses are assumed equal to the net yield stress, s_0. In this study, the following approximation is made:

$$\Omega = (1 - D) = \text{constant} \quad (4)$$

throughout the damage-zone. With this approximation, the HRR asymptotic solution near the crack-tip retains its classical singularity. It follows, after some algebraic manipulation, that the leading term of the displacement components, u_r and u_θ, in terms of polar coordinates (r,θ) measured from the crack tip can be expressed as:

$$u_r = \varepsilon_0 [\, J / (\varepsilon_0 \Omega s_0 \, I_n)]^{n/(n+1)} \; r^{1/(n+1)} \; \hat{\upsilon}_r (\theta) \quad (5a)$$

$$u_\theta = \varepsilon_0 [\, J / (\varepsilon_0 \Omega s_0 \, I_n)]^{n/(n+1)} \; r^{1/(n+1)} \; \hat{\upsilon}_\theta (\theta) \quad (5b)$$

where J is Rice's path independent integral, $\hat{\upsilon}_r (\theta)$ and $\hat{\upsilon}_\theta (\theta)$ are angular functions of the variable θ, and I_n is a constant of integration evaluated in [7] for different values of the strain-hardening parameter, n. For small-scale yielding solution, J is related to the elastic stress-intensity factor, K_I , by:

$$J = (1 - \nu^2) \, K_I^{\,2} / E \quad (6)$$

where E is Young's modulus and ν is Poisson's ratio. u_y The characteristic size, R, of the zone of dominance of the HRR singularity field depends strongly on hardening as demonstrated by Rice and Rosengren [6]. From the expressions of the Mises equivalent shear stress, τ, and shear strain, γ, the approximate distance from the crack-tip to the elastic-plastic boundary $R(\theta)$ is given by [6]:

$$\tau = \tau_0 \, [R(\theta) / r]^{1/(n+1)} \quad , \quad \gamma = \gamma_0 \, [R(\theta) / r]^{1/(n+1)} \quad (7)$$

where $R(\theta) = R(\theta;J,n)$ and τ_0 and γ_0 are yield stress and yield strain in shear, respectively. From equations (7), one immediately sees that $R(\theta)$ gives the shape of constant equivalent strain lines in the immediate vicinity of the crack-tip and that $R(\theta)$ can be interpreted as an approximate indication of the distance from the crack-tip to the elastic-plastic boundary.

In this paper, the HRR dominance region is assumed to represent the damage-zone, as within this region, plastic strains prevail and outside the zone, the component is predominantly elastic, considering small-scale yielding. For the fully-plastic condition, where the plastic zone reaches across the entire uncracked ligament, the validity zone ahead of the crack-tip is some small fraction of the uncracked ligament. In the case of the center-cracked tensile configuration, there is a much smaller zone of dominance, which becomes vanishingly small as $n \to \infty$. For light to medium hardening ($n \approx 10$), it was shown that the dominance zone is given, roughly, by: $R \approx 0.01$ b, where b is the length of the uncracked ligament, [8]. This paper is basically adhered to the small-scale yielding case in developing the fatigue crack propagation. However, for the onset of crack initiation in the fully-plastic range, the size of HRR dominance for the small-scale yielding, was considered for convenience and consistency of calculations.

Numerical solutions in small-scale yielding indicate that the HRR singularity fields provide a fairly good approximation out to distance ahead of the tip of roughly, [9]:

$$R = (0.2 \text{ to } 0.25) \, r_p \quad (8)$$

where r_p is the distance to the elastic-plastic boundary for linear-elastic fracture mechanics. According to Hutchinson, for small-scale yielding, it is readily verified, using the following formulas: $r_p = (1/3\,\pi) \, (K/\sigma_o)^2$, $R = 0.25 \; r_p$ and $J = (1 - \nu^2) \, K^2 / E$, that the condition for J-dominance, namely, $R > 3\delta_t$, is always satisfied, where δ_t is the crack-tip opening displacement. Expressing r_p in terms of the J-integral, for plane strain, yields:

$$r_p = (1/3\pi) \, [\, J / (\sigma_0)^2 \,] \, [\, E / (1 - \nu^2) \,] \quad (9)$$

Guided by the results of the anti-plane case, [4], the damage-zone in this paper is postulated as a circle of

radius ($0.25\ r_p$) centered at the crack-tip. Hence, it follows that the radius of the damage-zone is given as:

$$C = (1/ 12\pi s_0) (J / s_0) [E / (1 - \nu^2)] \Omega^{-2} \quad (10)$$

It should be noted that the size of the damage-zone given in equation (10) is not dependent on the strain-hardening exponent for the small-scale yielding solution. The effect of this independence will be addressed in the discussion of numerical results of crack instability criterion.

When the applied loading approaches the yield stress, large-scale yielding solution prevails. The displacement fields predicted from the HRR theory are reasonably accurate, despite the large plastic strains at the crack-tip [10]. The extension to large-scale yielding involves using the fully-plastic solution of a finite width panel containing a centered crack [11].

In the following, equations (1) through (10) are used to describe the conditions of the initiation of growth of the pre-existing crack due to monotonic loading and crack growth under cyclic loading.

3 Criterion for the onset of crack extension

The accumulated damage in the material is confined to a circular region, centered at the crack-tip, whose radius is given by equation (10). Inside the damage-zone, the tensile stress is given in terms of the effective stress:

$$\sigma_i = s [1 - \lambda u_i] \quad (11)$$

where u_i is the HRR displacement given by equations (5a) and (5b), for i = r and i = θ, respectively. In particular, equating the value of the exact tensile stress given by equation (11) to the approximate stress, Ωs, at (r, $\pi/4$), with r set equal to C in equation (10), yields:

$$(1- \Omega) = (\lambda s_0 / E) .[J / s_0] \Omega^{- [(n+2) / (n+1)]} G(n) \quad (12)$$

where,

$$G(n) = \varepsilon_0^{-1} .[I_n]^{-n / (n+1)} [12 \pi (1 - \nu^2)]^{-1/ (n+1)} . [\hat{u}_r(\pi/4) + \hat{u}_\theta(\pi/4)] \cos (\pi/4) \quad (13)$$

The measure of damage, D, is computed from the crack-tip opening displacement, 2 $u_r(C, \pi/2)$, which yields:

$$D = (\lambda s_0 / E) .[J / s_0] \Omega^{- [(n+2) / (n+1)]} H(n) \quad (14)$$

where,

$$H(n) = 2. \varepsilon_0^{-1} . [I_n]^{-n / (n+1)} [12 \pi (1 - \nu^2)]^{-1/ (n+1)} [\hat{u}_r(\pi/2)] \quad (15)$$

The criterion for the onset of crack extension is established by requiring D(C, $\pi/2$) in equation (14) to approach unity and using equation (12) to eliminate the continuity function, Ω. The result is:

$$(\lambda s_0 / E).[J / s_0] = \{1 - [G(n)/H(n)]\}^{(n+2) / (n+1)} / H(n) \quad (16)$$

In the remaining part of this section, equation (16) is used to predict the onset of crack growth for external loading characterized by the small-scale yielding and the fully-plastic solution.

3.1 Small-scale Yielding Solution

For small-scale yielding, the J-integral is replaced by the elastic stress-intensity factor, namely, $J = (1 - \nu^2) K_I^2 / E = \pi (1 - \nu^2) \sigma_\infty^2 a_0 / E$. Substituting in equation (16), the following condition for the initiation of crack growth is obtained:

$$(\lambda s_0 a_0 / E) .[\pi (1 - \nu^2) \varepsilon_0] (\sigma_\infty / s_0)^2 = \{1 - [G(n)/H(n)]\}^{(n+2) / (n+1)} / H(n) \quad (17)$$

In order for small-scale yielding to be valid, (σ_∞ / s_0) has to be less than about 0.5. It is clear that equation (17) confirms Griffith's classical result, namely, σ_∞ is proportional to $a_0^{-.5}$. The constant of proportionality in equation (17) is a material parameter. Similar result was obtained for the small-scale yielding solution for the anti-plane mode case, [4].

3.2 Large-scale Yielding Solution

The extension to large-scale yielding involves using the fully plastic solution for Rice's J-integral in equations (12) and (14). It is realized that the damage-zone extension in the fully plastic range will be much smaller than that of the small-scale yielding. However, for simplicity of calculations, the damage-zone extension in large-scale yielding is assumed to be the same as that postulated in the previous section for small-scale yielding. The fully plastic J for the damaged material can be obtained along the same lines outlined in [11]. For a crack of length $2a_0$, in an infinite strip of width, 2W, subjected to a constant stress, σ_∞, at the remote boundary, under fully-plastic conditions, it can be shown that:

$$J / s_0 = (s_0 a_0 / E) (\sigma_\infty / s_0)^{n+1} (b/w) h_1 (n) \Omega^{-n} \quad .....(18)$$

where Ω is given in equation (12) and h_1 (n) is a function of the strain-hardening exponent and geometry, whose numerical values, for (a/W) = 0.125, are given in Table 1.

Upon eliminating S from equation (12) using (18), it follows that the onset of crack growth ensues when:

$$(8 s_0 a_0 / E) (F_4 / s_0)^{(n+1)} [g_0 (b/w) h_1 (n)] = \{1 - [G(n)/H(n)]\}^m / H(n) \quad .....(19)$$

where the superscript, m, is given by: $m = (n^2+2n+2) / (n+1)$.

Equation (19) shows that σ_∞ is proportional to $a_0^{-1/(n+1)}$, which is identical to the result obtained by Mahmoud and Kassir for the anti-plane crack, [4]. Equation (19) is valid for values of σ_∞ / s_0 in the range 0.5 to 1.0. The variation of the critical loads with crack length predicted by equations (17) and (19) are shown in Figure 1, at a value of $\lambda = 10^6$ in^{-1} (39,370 mm^{-1}). Equation (17) reveals the variation of the critical stress with crack length for $\sigma_\infty / s_0 < {}^1/_2$, while equation (19) exhibits the behavior for ${}^1/_2 < \sigma_\infty / s_0 < 1.0$. In the small-scale yielding domain, the critical stress is proportional to the square root of the crack length and the strain-hardening of the material plays insignificant role. In contrast, the influence of the strain-hardening exponent is demonstrated in the fully plastic range. It is clear from Figure 1 that the external load required to cause instability decreases with increasing values of the hardening exponent n. As the crack length increases, lower external load is required to cause failure. Another noteworthy feature about the developed criterion is the effect of Poisson's ratio, ν, on the crack extension. Figure 2 exhibits the instability curve corresponding to a strain-hardening exponent, n = 20, for two different values of Poisson's ratio, namely, ν = 0.0 and ν = 0.5. The influence of Poisson's ratio, ν, on the fully-plastic solution is by no means significant. However, Figure 2 shows a more pronounced influence of ν on the small-scale yielding range of the curve. It is also clear from

Table 1. Numerical values of h_1 (n) in equation (18)

n	h_1 (n)
1	2.8
2	3.61
3	4.06
5	4.35
7	4.33
10	4.02
13	3.56
16	3.06
20	2.46

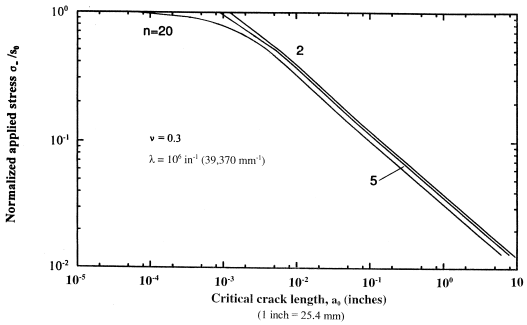

Figure 1. Variation of the applied stress, σ_∞ / S_0, with crack lenth, a_0.

the figure that the higher value of Poisson's ratio, namely, $\nu = 0.5$ corresponds to a higher value of the crack length at instability compared with $\nu = 0.0$, for the same load ratio and (hypothetically) the same material parameter. This result is expected, as higher value of Poisson's ratio reflects higher ductility of the material and larger capacity to sustain plastic deformation imposed by the damage process.

4 Fatigue crack propagation

Fatigue crack propagation under cyclic tensile loading is studied in this section. Each loading cycle contains an increase varying from 0 to σ_∞, which imposes an instantaneous damage increment, ΔD, proportional to the normal displacement, within the damage-zone. No damage is caused upon loading from σ_∞ to 0, to comply with the deformation theory. No hold time effects are considered in the present analysis. Interest is, rather, focused on the effect of load changes. Analysis is adhered to the small-scale yielding solution. In the following calculations, r is set equal to C given in equation (10). Denoting by D(r, $\pi/2$), the damage at a point (r, $\pi/2$) from the crack_tip, it follows that after N load cycles:

$$D(C, \pi/2; N) = D(C, \pi/2: -1) + \eta . u_r(C, \pi/2; N) \quad (20)$$

where η is a material damage parameter and D(C, $\pi/2$; N) is a function of the continuity function, Ω.
To obtain a value of the continuity function, Ω, the exact and the approximate stresses are set equal at (C, $\pi/4$), i.e.

$$\Omega(N) = 1 - D(C, \pi/4 ; N) \quad (21)$$

where now D(C, $\pi/4$; N) is given by:

$$D(C, \pi/4 ; N) = D(C, \pi/4 ;N-1) + \eta.[u_r(C, \pi/4 ;N) + u_\theta(C, \pi/4 ;N)] (1/\sqrt{2}) \quad (22)$$

Combining equations (5), (13), (21), and (22), one can write:

$$\Omega(N) = 1 - (\eta s_0 a_0 / E) .[\pi (1 - \nu^2) \varepsilon_0]^{n/(n+1)} (\sigma_\infty/s_0)^2 G(n) .\{[\Omega^{-[(n+2)/(n+1)]} (N-1)] + [\Omega^{-[(n+2)/(n+1)]} (N)]\} \quad (23)$$

For N = 0, there is no damage and Ω=1, while corresponding to N = 1, there is instantaneous damage accumulated in the damage-zone, whereby, the extent of the zone and the crack opening displacement within the zone can be evaluated. The extent of the damage-zone ahead of the crack-tip is obtained from equation (10) as:

$$C(N) = (1/12\pi) (K_I /\Omega(N) s_0)^2 \quad (24)$$

For each cycle of loading, $u_r(C, \pi/2)$, $u_r(C, \pi/4)$, $u_\theta(C, \pi/4)$,$\Omega(N)$ and C(N), are calculated using equations (5) and (21)-(24).
The new crack length, a, which is found from the condition:

$$D(a_N , N) = 1 \quad (25)$$

is incrementally computed from:

$$a_N = a_0 + da_N \quad (26)$$

where:

$$da_N = [1 - \{1/ D(r, \pi/2;N)\}] C(N) \quad (27)$$

Using the new crack length given by equations (26) and (27), the iterative process can be repeated to obtain the final values of a(N), C(N), w(r, θ ;N), D(r, θ ;N) and Ω(N) at which instability is reached, i.e., the critical crack length to cause crack instability is reached.
The influence of the strain-hardening exponent has been numerically studied to demonstrate the effect of different material parameters on crack propagation due to the fatigue process. Figures 3 and 4 exhibit the influence of different stress levels on the loading cycles for different values of the strain-hardening exponent. It is

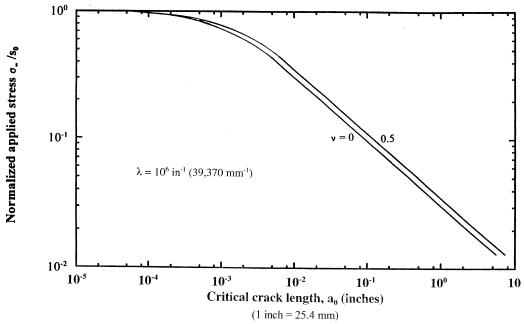

Figure 2. Influence of Poisson's ratio on crack extension for n=20.

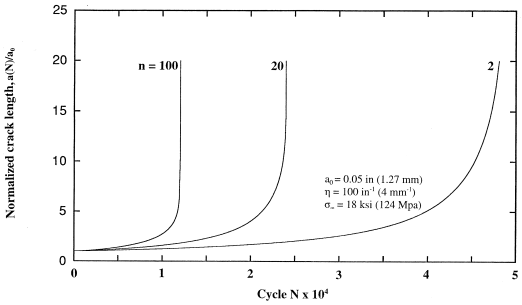

Figure 4. Strain hardening variation with crack growth at σ_{∞} = 18 ksi (124 Mpa) and η=100 in^{-1} (4 mm^{-1}).

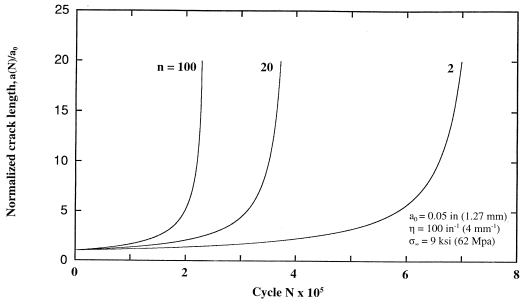

Figure 3. Crack growth due to cyclic loading at σ_{∞} = 9 ksi (62 Mpa) and η=100 in^{-1} (4 mm^{-1}).

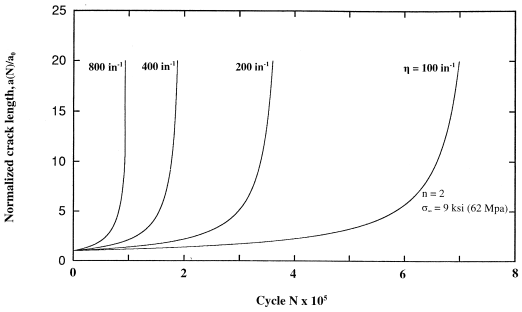

Figure 5. Material damage parameter's influence on fatigue crack growth at σ_{∞} = 9 ksi (62 Mpa), for n=2.

clear from these figures that the number of load cycles required to cause failure decreases with increasing values of the strain-hardening exponent and the applied stress. Figure 5 displays the variation of the normalized crack length, a(N) / a_0, and the number of cycles required for failure under different values of the material parameters, at constant stress level and n = 2. For decreasing value of the material parameter, which indicates reduced level of damage, the number of load cycles required for failure increases. Figure 6 shows the relationship between the normalized length of the crack, a(N) / a_0, and the number of loading cycles corresponding to different levels of the applied load at a constant material parameter and n = 2. As expected: the number of load cycles required to cause failure decreases for higher values of the applied load. It is noted that Figures 3 through 6, typically, display an

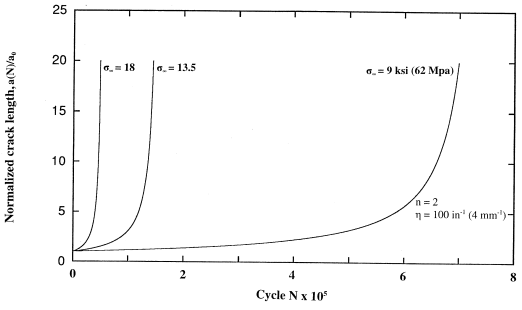

Figure 6. Influence of external stress ratio, σ_{∞/S_0} ,on fatigue crack growth at η=100 in^{-1} (4 mm^{-1}) for n=2.

incubation period, within which damage accumulates without crack growth, ending with onset of crack growth that triggers a growth period, which is terminated by failure at a certain number of cycles of loading.

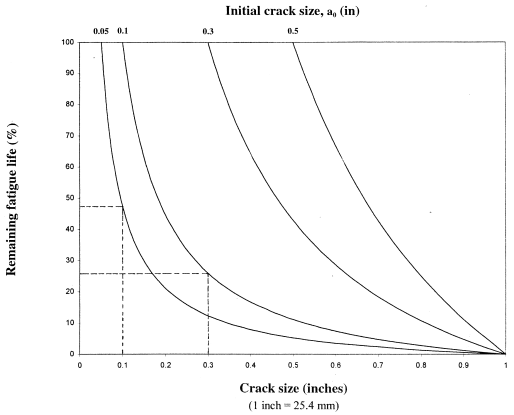

Figure 7. Effect of initial crack size, a_0, on remaining fatigue life.

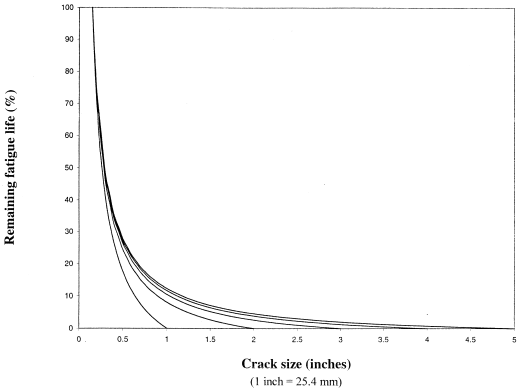

Figure 8. Effect of final crack size, a_f, on remaining fatigue life.

In the remaining of this section, the effect of initial and final crack size in addition to the effect of cyclic stress level on the fatigue life of a welded steel bridge component are demonstrated.

4.1 Effect of Initial Crack Size

To illustrate the effect of initial crack size, the remaining fatigue life, $N = N_f - N_i$, as predicted from the damage model is plotted versus initial crack size in Figure 7. As shown in the figure, if the initial crack size is increased from 0.05 inch (1.27 mm) to 0.1 inch (2.54 mm), the remaining life reduces by about 50% of the life for a 0.05-inch (1.27 mm) initial crack. Then, for instance, if the weld quality were such that the crack size that cannot be detected is 0.1-inch (2.54 mm) instead of .05-inch (1.27 mm), half of the fatigue life would be consumed, by allowing larger initial cracks to remain in the structure. If the final crack size is taken to be the same and equal to 1 inch (25.4 mm), one can see that a threefold increase in initial crack size from 0.1-inch (2.54 mm) to 0.3-inch (7.62 mm) reduces the remaining life to about 25%. This demonstrates the strong effect of initial crack size on bridge life and emphasizes the importance of taking into account the quality of initial crack size in the prediction of fatigue life of welded bridges subjected to cyclic loading.

4.2 Effect of Final Crack Size

The influence of final crack size on fatigue life is demonstrated by plotting the remaining fatigue life versus final crack size using an initial crack size of 0.15 inch (3.81 mm), as shown in Figure 8. In this figure, a final crack size ranging from one inch (25.4 mm), which is used for Figure 7, to 5 inches (127 mm) has been used. Only marginal increases in remaining life are obtained for quite substantial changes in final crack size. For instance, an increase in final crack size from one inch (25.4 mm) to two inches (50.8 mm) results in a mere 7% increase in remaining life and an increase from one inch (25.4 mm) to 5 inches (127 mm) yields only about 12% in remaining fatigue life. This illustrates that the final crack size has little effect on bridge life when the controlling failure mechanism is fatigue.

4.3 Effect of Cyclic Stress Level

Using Paris power law, the rate of fatigue crack growth, da/dN, is given by:

$$da/dN = C_p (\Delta K)^p \quad (28)$$

where ΔK is the stress intensity factor range, and C_p and p are material parameters. A growth exponent, p, of four is appropriate for most welded steel structures,

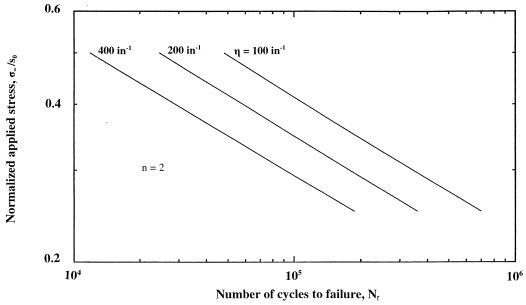

Figure 9. Number of cycles to failure Nf, versus external stress ratio, σ_{∞}/S_0 .

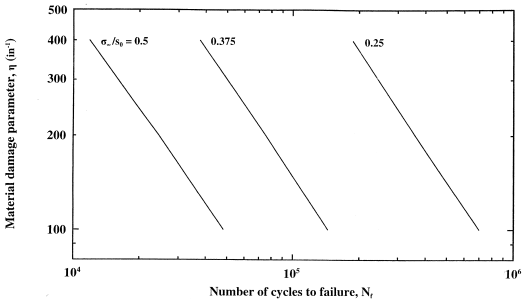

Figure 10. Number of cycles to failure Nf, versus material damage parameter, η.

[12]. The stress intensity factor range ΔK in this case is $\Delta K = \sigma_{\infty} \sqrt{\pi a}$. Then, the number of cycles required to cause failure, N_f, may, therefore, be expressed as:

$$N_f = [a_i]^{1 - p/2} \ \sigma_{\infty}^{-p} \ / [1 - p/2] \ [C_p \ \pi^{p/2}] \ \text{.....(29)}$$

From this equation, one observes that $N_f \propto \sigma_{\infty}^{-p}$. With p = 4, Figure 9 predicts that $N_f \propto \sigma_{\infty}^{-3.9}$ which is in very good agreement with the prediction of equation (29). One more noteworthy feature of Figure 9 is that different values of the material damage parameter, η, could be looked at as indicator of the category of the weld detail, i.e. Category D, E, E' or F as defined by the AASHTO Specifications, with the worst case corresponding to the highest value of η reflecting severer state of damage. It is also noted that equation (29) predicts the relation: $N_f \propto a_i^{-1}$, which is in good agreement with the results shown in Figure 10, for different values of the external stress, σ_{∞}.

Using equation (29), and assuming that the cyclic stress is reduced by a factor of two, the initial crack size that would give the same predicted service life is given by:

$$a_{i\,(0.5\,\sigma\infty)} = a_{i\,(\sigma\infty)} \ [16\ a_f / (\ a_f + 15\ a_i\ )] \text{.....(30)}$$

Since $0 < a_i < a_f$, numerical values of the above formula range between one and 16. For high cycle fatigue in welded bridges, $a_f >> a_i$. Thus, a 16-fold increase in initial crack size can result if stresses are reduced by a factor of two. The same 16-fold increase in number of cycles required to cause failure is also predicted by equation (20), when the stress is reduced by a factor of two. This is in a very good agreement with the average 15.5-fold increase, predicted by the damage model as shown in Figures 3 and 4.

5 Conclusions

A continuum damage model is used to study fracture behavior of steel bridge components subjected to Mode-I loading. The model is based on interaction between a macroscopic crack and the uniformly distributed damage ahead of its tip. A damage parameter is incorporated in the HRR asymptotic solution to describe the stress and displacement fields in the vicinity of the crack-tip for a power-law hardening material. For monotonic loading, the external stress is shown to be proportional to $a_0^{-1/(n+1)}$, which reduces to Griffith's classical result for elastic material. For fatigue crack growth, it is shown that the initial crack size has a strong influence on bridge life and that the initial weld quality is of a paramount importance in the prediction of fatigue life of welded bridges subjected to cyclic loading. On the other hand, final crack size has very little influence on total bridge life. It is also found that if the applied stress is reduced by a factor of two, a 15.5-fold increase in number of cycles elapsed to failure is gained, which is in a good agreement with the

16-fold increase predicted by Paris power-law for fatigue crack growth. Finally, the main conclusion of this paper is that the proposed continuum damage model describes the fracture behavior of steel bridge components very well and seems as a promising tool in the prediction of bridge life.

REFERENCES

[1] Fisher, J. W., Yen, B. T. and Dayi, W. (1989). *Fatigue of Bridge Structures- A Commentary and Guide for Design, Evaluation and Investigation of Cracking*. ATLSS Report No. 89-02.

[2] Kachanov, L.M. (1958). Time of the Rupture Process under Creep Conditions." *Izv. Akad. Nauk SSSR.* Otd*. Tekh. Nauk*, 8, 26-31.

[3] Mahmoud, K. M. (1997). *Continuum Damage Model For Plastic Fracture of Work-Hardening Materials.* Ph.D. Dissertation, The City University of New York.

[4] Mahmoud, K. M. and Kassir, M. K. (1998). "Damage Accumulation Due to Growth of An Anti-Plane Crack in a Work-Hardening Material." *Theoretical and Applied Fracture Mechanics,* Vol. 29, pp. 41-48, 1998.

[5] Hutchinson, J. W. (1968). "Singular Behavior at The End of a Tensile Crack in a Hardening Material." *Journal of the Mechanics and Physics of Solids*, 16, 13-31.

[6] Rice, J. R. and Rosengren, G. F. (1968). "Plane Strain Deformation Near a Crack Tip in a Power-Law Hardening Material." *Journal of the Mechanics and Physics of Solids*, 16, 1-12.

[7] Shih, C. F. (1983). "Tables of Hutchinson-Rice-Rosengren Singular Field Quantities." *Brown University Report* MRL E-147.

[8] McMeeking, R. M. and Parks, D. M. "On Criteria for J Dominance of Crack tip Fields in Large Scale Yielding," ASTM STP 668, pp. 175-194, 1979.

[9] Hutchinson, J. W. (1983). "Fundamentals of the Phenomenological Theory of Nonlinear Fracture Mechanics." *Trans. of the ASME*, 50, 1042-1051.

[10] Shih, C. F. (1981). "Relationship Between the J-Integral and The Crack Opening Displacement for Stationary and Extending Cracks." *Journal of the Mechanics and Physics of Solids,* 29, 305-326.

[11] Kumar, V., German, M. D. and Shih, C.F. (1981). "An Engineering Approach for Elastic-Plastic Fracture Analysis." EPRI Report NP-1931, *Electric Power Research Institute, Palo Alto, Ca.*

[12] Maddox, S. J. (1969). "Fatigue Crack Propagation in Weld Metal and Heat Affected Zone Material." *Welding Institute Report* E/29/69, 1969.

Appendix: Notation

The following symbols are used in this paper:

A = original cross-sectional area.
A_{net} = net cross-sectional area.
A_{void} = cross-sectional area occupied by voids.
a = crack length.
a_0 = initial crack length.
$a(N)$ = crack length at load cycle N.
$a(t)$ = crack length at time t.
b = length of uncracked ligament.
C = plastic zone extension ahead of the crack-tip.
C_P = material parameter.
D = damage variable.
E = Young's modulus of elasticity.
$G(n)$ = strain-hardening dependent constant at 2 = B/4.
$H(n)$ = strain-hardening dependent constant at 2 = B/2.
$h_1(n)$ = strain-hardening dependent function.
I_n = integration constant for Mode-I.
J = Rice's contour integral.
K_I = Mode-I elastic stress-intensity factor.
m = strain-hardening dependent constant.
n = strain-hardening exponent of the material.
p = material parameter.
N = number of loading cycles.
N_f = number of loading cycles required for failure.
N_i = number of loading cycles required for the onset of crack growth.
R = radius of the zone of dominance of the HRR field.
r_p = distance to the elastic-plastic boundary.
s = effective stress.
s_0 = effective yield stress of the material.
$\mathbf{u}$ = in-plane displacement vector.
W = width of a structural strip subject to in-plane loading.
x,y,z = cartesian coordinates.
γ = shear strain.
γ_0 = yield strain in shear.
ΔD = damage increment.
ΔK = stress intensity factor range.
δ_t = crack-tip opening displacement (CTOD).
η = damage parameter for cyclic loading.
θ = angle measured from the crack-tip.
λ = damage parameter for monotonic loading.
ν = Poisson's ratio of elastic contraction.
σ_{ij} = stress tensor.
σ_0 = yield stress in tension.
σ_∞ = remotely applied in-plane tensile stress.
τ = shear stress.
τ_0 = yield stress in shear.
Ω = continuity function of damage.
ε_0 = yield strain in tension.
$\hat{\upsilon}_r(\theta)$ = angular function of the variable θ, with respect to r.
$\hat{\upsilon}_r(\theta)$ = angular function of the variable θ, with respect to θ.